

Effect of Phase Factor in the Geometric Entanglement Measure of Three-Qubit States

Sayatnova Tamaryan

Theory Department, Yerevan Physics Institute, Yerevan-36, 375036, Armenia

Hungsoo Kim

The Institute of Basic Science, Kyungnam University, Masan, 631-701, Korea

Mu-Seong Kim, Kap Soo Jang, DaeKil Park

Department of Physics, Kyungnam University, Masan, 631-701, Korea

Abstract

Any pure three-qubit state is uniquely characterized by one phase and four positive parameters. The geometric measure of entanglement as a function of state parameters can have different expressions. Each of expressions has its own applicable domain and thus the whole state parameter space is divided into subspaces that are ranges of definition for corresponding expressions. The purpose of this paper is to examine the applicable domains for the most general qubit-interchange symmetric three-qubit states. First, we compute the eigenvalues of the non-linear eigenvalue equations and the nearest separable states for the permutation invariant three-qubit states with a fixed phase. Next, we compute the geometric entanglement measure, deduce the boundaries of all subspaces, and find allocations of highly and slightly entangled states. It is shown that there are three applicable domains when the phase factor is $\pi/2$ while other cases have only two domains. The emergence of the three domains is due to the appearance of the additional W-state. We show that most of highly entangled states reside near the boundaries of the domains and states located far from the boundaries become less-entangled and eventually go to the product states. The neighbors of W-state are generally more entangled than the neighbors of Greenberger-Horne-Zeilinger(GHZ) state from the aspect of the geometric measure. However, the range of the GHZ-neighbors is much more wider than the range of the W-neighbors.

I. INTRODUCTION

Entanglement is a property of quantum states that does not exist classically. Two or more subsystems of a quantum system are said to be entangled if the state of the entire system cannot be described in terms of a state for each of the subsystems [1]. This property of composite quantum systems, which exhibits quantum correlations between subsystems, is a resource for many processes in quantum information theory [2, 3, 4, 5]. Since the profound measures of entanglement, i.e. the entanglement of formation and distillation [6, 7, 8, 9], have not been properly generalized to multipartite systems, the study of quantifying multipartite entanglement via other measures [10, 11, 12, 13, 14] is a necessity.

The entanglement of a given pure state can be characterized by a distance to the nearest unentangled state [15]. A whole class of such entanglement monotones, based on the Euclidean distance of a given multipartite state to the nearest fully separable state, was constructed in Ref.[16]. Subsequently, a geometrically motivated measure of entanglement, known as geometric measure, was introduced by Wei and Goldbart [17]. It is a decreasing function of the maximal overlap P_{max} and is suitable for any partite system regardless of its dimensions. The maximal overlap has several different names and we list all of them for the completeness: maximal probability of success [13], entanglement eigenvalue [17], injective tensor norm [18], the largest Schmidt coefficient [19] and maximum singular value [20].

The geometric measure has an advantage that it can be computed analytically for multi-parameter states. Recently, explicit expressions for the maximal overlap have been derived for three-[17, 20, 21, 22, 23] as well as for multi-qubit states [24, 25, 26, 27]. It turned out that the maximal overlap, depending on coefficients of a quantum state in a computational basis, can take two different values. It is equal to either the square of the largest coefficient or the square of the circumradius of a cyclic polygon constructed by the coefficients of the quantum state. This means that the whole parameter space is divided into two subspaces each of which has its own expression for the geometric measure.

In spite of these achievements, still we lack sufficient knowledge to classify generic three-qubit pure states by the geometric measure. They have five local unitary(LU) invariants including four positive parameters and a gauge phase γ [19, 28, 29]. The maximal overlap of these states is not known yet. Only three-qubit states which are expressed as linear combinations of four(or less) orthogonal product states have been considered so far [22].

In fact, all of these states have real coefficients because the phases of their coefficients can be eliminated by LU-transformations. Thus, the contribution of the gauge phase to the maximal overlap has remained a mystery. On the other hand, the most recent results [30] have shown that the gauge phase plays an important role. It parameterizes the family of maximally entangled states and identifies W-class pure states with the boundary of pure states.

In this paper we would like to take into complete account the effect of the gauge phase in the geometric measure of entanglement. We compute the maximal overlap as well as the nearest product states for a given value of the gauge phase. We will show in the following that depending on the phase factor γ the whole parameter space is divided into the two or three domains, each of which has a particular expression for the geometric measure. In addition, we will show that most of highly entangled states reside near the boundaries of the domains. We will call these highly entangled states as GHZ-neighbors. The states located far from the boundaries become less-entangled and eventually go to the product states. But there is different kind of the highly entangled states. These states reside around W-states. We will call these highly entangled states as W-neighbors. The W-neighbors are generally more entangled than the GHZ-neighbors from the aspect of the geometric measure. However, the range of the GHZ neighbors is much more wider than the range of the W-neighbors.

The paper is organized as follows. In section II following Ref.[21] we transform the nonlinear eigenvalue equations into the Lagrange multiplier equations. In section III we solve the Lagrange multiplier equations analytically for $\gamma = 0$ and $\gamma = \pi/2$. It turns out that both cases give five different eigenvalues. Also every eigenvalue has its own available region in the parameter space. In section IV we compute the geometric measure for $\gamma = 0$ case. It turns out that two of the five eigenvalues contribute to the geometric measure. This means that the whole parameter space is divided into two applicable domains. In section V we compute the geometric measure for $\gamma = \pi/2$ case. It is shown that the whole parameter space is divided into the three applicable domains. In section VI we compute the eigenvalues and the geometric measure for $\gamma = \pi/4$ numerically. It is shown that when $\gamma = \pi/4$, there are six different eigenvalues. However, only two eigenvalues contribute to the geometric measure. In section VI a brief conclusion is given. In appendix we have shown that Lagrange multiplier equations for arbitrary γ provides a solution whose multiplier constant is zero.

II. GENERAL FORMALISM

In this section we clarify our notations, give necessary definitions, define three-qubit symmetric states and transform nonlinear stationarity equations to a system of linear equations.

A. Preliminaries

The maximal overlap of n -qubit pure states is given by

$$P_{max} = \max_{q_1, q_2, \dots, q_n} |(\langle q_1 | \otimes \langle q_2 | \otimes \dots \otimes \langle q_n |) | \psi \rangle|^2, \quad (2.1)$$

where the maximization is performed over single qubit pure states. Constituents $|q_1\rangle, |q_2\rangle, \dots, |q_n\rangle$, the nearest product state from $|\psi\rangle$, can be computed via the non-linear eigenvalue equations

$$\langle q_1 | \dots \langle q_{n-1} | \psi \rangle = \mu_i |q_n\rangle, \langle q_1 | \dots \langle q_{n-2} | \langle q_n | \psi \rangle = \mu_i |q_{n-1}\rangle, \dots, \langle q_2 | \dots \langle q_n | \psi \rangle = \mu_i |q_1\rangle, \quad (2.2)$$

where μ_i 's are the eigenvalues of Eq.(2.2). Then the geometric measure G of the quantum state $|\psi\rangle$ is defined as $G(\psi) = 1 - P_{max}$, where $P_{max} = \max(\mu_i^2)$.

For simplicity, we take a quantum states which possess a permutational symmetry [31, 32, 33]. These states have three independent parameters and, through an appropriate LU transformations, can be brought into the symmetric form [19]

$$|\psi\rangle = g|000\rangle + t|011\rangle + t|101\rangle + t|110\rangle + e^{i\gamma}h|111\rangle, \quad (2.3)$$

where we follow the notation of Ref.[30]. In above equation all coefficients g , h and t are positive and satisfy the normalization condition $g^2 + 3t^2 + h^2 = 1$. The phase γ has the period π and ranges within the interval $-\pi/2 \leq \gamma \leq \pi/2$. Note that Eq.(2.3) is not a Schmidt decomposition for $|\psi\rangle$ since the Schmidt normal form imposes additional conditions (namely, a lower bound on g) on state parameters. We would like to abandon these additional constraints and apply the general method proposed in Ref.[21] to symmetric states Eq.(2.3).

B. Modified stationarity equations

In this subsection we would like to present the method for solving stationarity equations for the quantum state given in Eq.(2.3). In the case of three-qubit pure states the method

developed in Ref.[21] transforms the system of nonlinear equations to a system of linear equations. In spite of this essential simplification, it is impossible to get analytic expressions for generic three-qubit states since the solution of the linear eigenvalue equations reduces to the root finding for a couple of algebraic equations of degree six [22]. However, the permutation symmetry of $|\psi\rangle$ reduces this pair of algebraic equations to a single algebraic equation of degree six. Furthermore, there is a solution which holds for all values of state parameters [30]. The separation of this global solution allows us to solve explicitly the eigenvalue equations for $\gamma = 0$ and $\gamma = \pi/2$ and leads us to a quartic equation for remaining cases. The quartic is the highest order polynomial equation that can be solved by radicals in the general case. But expressions for roots are impractical and we will carry out numerical analysis instead.

The method enables us to express eigenvalues μ^2 via the reduced densities ρ^A , ρ^B and ρ^{AB} of qubits A and B in a form:

$$\mu^2 = \frac{1}{4} \max_{|\mathbf{s}_1|=|\mathbf{s}_2|=1} (1 + \mathbf{r}_1 \cdot \mathbf{s}_1 + \mathbf{r}_2 \cdot \mathbf{s}_2 + G_{ij} s_{1i} s_{2j}), \quad (2.4)$$

where

$$\mathbf{r}_1 = \text{Tr}(\rho^A \boldsymbol{\sigma}), \quad \mathbf{r}_2 = \text{Tr}(\rho^B \boldsymbol{\sigma}), \quad G_{ij} = \text{Tr}(\rho^{AB} \sigma_i \otimes \sigma_j) \quad (2.5)$$

and σ_i 's are Pauli matrices. Explicit calculation shows

$$\begin{aligned} \mathbf{r} \equiv \mathbf{r}_1 = \mathbf{r}_2 &= (2ht \cos \gamma, 2ht \sin \gamma, g^2 - h^2 - t^2) \\ G_{ij} &= \begin{pmatrix} 2t(g+t) & 0 & -2ht \cos \gamma \\ 0 & -2t(g-t) & -2ht \sin \gamma \\ -2ht \cos \gamma & -2ht \sin \gamma & g^2 + h^2 - t^2 \end{pmatrix}. \end{aligned} \quad (2.6)$$

It is worthwhile noting that \mathbf{r}_1 is identical with \mathbf{r}_2 and G_{ij} is a symmetric matrix. These properties arise due to the fact that we have chosen the symmetric state in Eq.(2.3) under the qubit-exchange. As will be shown in the following these properties drastically simplify the calculation procedure. Since \mathbf{r}_1 , \mathbf{r}_2 and G_{ij} are explicitly derived, the eigenvalues μ^2 can be computed if \mathbf{s}_1 and \mathbf{s}_2 are known. Due to the maximization in Eq.(2.4) these vectors can be computed by solving the Lagrange multiplier equations:

$$\mathbf{r}_1 + G \mathbf{s}_2 = \lambda_1 \mathbf{s}_1 \quad \mathbf{r}_2 + G^T \mathbf{s}_1 = \lambda_2 \mathbf{s}_2 \quad (2.7)$$

where the superscript T stands for transpose and λ_i 's are the Lagrange multiplier constants. From the properties $\mathbf{r}_1 = \mathbf{r}_2$ and $G_{ij} = G_{ji}$ Eq.(2.7) can be reduced to a single equation

$$\mathbf{r} + G\mathbf{s} = \lambda\mathbf{s} \quad (2.8)$$

where $\lambda \equiv \lambda_1 = \lambda_2$ and $\mathbf{s} \equiv \mathbf{s}_1 = \mathbf{s}_2$. Letting

$$\mathbf{s} = (\sin \theta \cos \varphi, \sin \theta \sin \varphi, \cos \theta), \quad (2.9)$$

Eq.(2.8) reduces to

$$2ht \cos \gamma + 2t(g+t) \sin \theta \cos \varphi - 2ht \cos \gamma \cos \theta = \lambda \sin \theta \cos \varphi \quad (2.10a)$$

$$2ht \sin \gamma - 2t(g-t) \sin \theta \sin \varphi - 2ht \sin \gamma \cos \theta = \lambda \sin \theta \sin \varphi \quad (2.10b)$$

$$(g^2 - t^2)(1 + \cos \theta) - h^2(1 - \cos \theta) - 2ht \cos \gamma \sin \theta \cos \varphi - 2ht \sin \gamma \sin \theta \sin \varphi = \lambda \cos \theta. \quad (2.10c)$$

Solving θ , φ and λ from Eq.(2.10), one can compute the eigenvalues for the symmetric canonical state (2.3) by inserting the solutions into Eq.(2.4). In the next section we will solve analytically Eq.(2.10) at the particular phases $\gamma = 0$ and $\gamma = \pi/2$. By making use of the solutions we will compute μ_i and $P_{max} = \max(\mu_i^2)$ for the corresponding quantum states.

III. EIGENVALUES

In this section Eq.(2.10) will be solved at $\gamma = 0$ and $\pi/2$ separately. Since numerical calculation is needed to analyze the $\gamma = \pi/4$ case, we deal with this case in different section (see section VI).

A. $\gamma = 0$ case

For this case Eq.(2.10) reduces to

$$2t(g+t) \sin \theta \cos \varphi + 2ht(1 - \cos \theta) = \lambda \sin \theta \cos \varphi \quad (3.1a)$$

$$-2t(g-t) \sin \theta \sin \varphi = \lambda \sin \theta \sin \varphi \quad (3.1b)$$

$$(g^2 - t^2)(1 + \cos \theta) - h^2(1 - \cos \theta) - 2ht \sin \theta \cos \varphi = \lambda \cos \theta. \quad (3.1c)$$

Eq.(3.1b) implies that the solutions for the $\gamma = 0$ case are categorized by $\theta = 0$, $\varphi = 0$, $\varphi = \pi$ and $\lambda = -2t(g - t)$ ¹.

1. $\theta = 0$ case

When $\theta = 0$, Eq.(3.1a) and Eq.(3.1b) are automatically solved, and Eq.(3.1c) gives

$$\lambda = 2(g^2 - t^2). \quad (3.2)$$

Now $\mathbf{s} = (0, 0, 1)$ and Eq.(2.4) together with the normalization condition $g^2 + 3t^2 + h^2 = 1$ gives the eigenvalue

$$\mu_P^2 = g^2. \quad (3.3)$$

2. $\varphi = 0$ case

For this case Eq.(3.1b) is automatically solved and the remaining equations are

$$2t(g + t) \sin \theta + 2ht(1 - \cos \theta) = \lambda \sin \theta \quad (3.4a)$$

$$(g^2 - t^2)(1 + \cos \theta) - h^2(1 - \cos \theta) - 2ht \sin \theta = \lambda \cos \theta. \quad (3.4b)$$

Since $\sin(\theta/2) \neq 0$, Eq.(3.4a) reduces to

$$\lambda = 2htz + 2t^2 + 2tg \quad (3.5)$$

where $z = \tan(\theta/2)$. Inserting Eq.(3.5) into Eq.(3.4b), one can derive an equation

$$(hz + g + t)(tz^2 - hz + g - 2t) = 0. \quad (3.6)$$

Eq.(3.6) implies that the $\varphi = 0$ case is also categorized again by following three cases:

$$z = -\frac{g + t}{h}, \quad \frac{r_+}{2t}, \quad \frac{r_-}{2t} \quad (3.7)$$

where

$$r_{\pm} = h \pm \sqrt{h^2 + 4t(2t - g)}. \quad (3.8)$$

¹ The case $\theta = \pi$ can be excluded by Eq.(3.1a).

First, let us consider the case of $z = -(g+t)/h$. In this case Eq.(3.5) gives

$$\lambda = 0. \quad (3.9)$$

Since, in this case,

$$s_x = \sin \theta = -\frac{2h(g+t)}{h^2 + (g+t)^2}, \quad s_y = 0, \quad s_z = \frac{h^2 - (g+t)^2}{h^2 + (g+t)^2}, \quad (3.10)$$

it is straightforward to compute the eigenvalues for this case, which is

$$\mu_1^2 = \frac{g^2 h^2 + t^2 (g+t)^2}{h^2 + (g+t)^2}. \quad (3.11)$$

Next, let us consider the case of $z = r_{\pm}/2t$ simultaneously. In these cases Eq.(3.5) gives

$$\lambda = hr_{\pm} + 2t(g+t). \quad (3.12)$$

Since, in these cases,

$$s_x = \frac{4tr_{\pm}}{r_{\pm}^2 + 4t^2}, \quad s_y = 0, \quad s_z = -\frac{r_{\pm}^2 - 4t^2}{r_{\pm}^2 + 4t^2}, \quad (3.13)$$

one can show directly that the eigenvalues are

$$\mu_{\pm}^2 = \frac{(hr_{\pm} + 4t^2)^2}{r_{\pm}^2 + 4t^2}. \quad (3.14)$$

Since $z = \tan(\theta/2)$ should be real, the eigenvalues μ_{\pm}^2 are available only when

$$g \leq 2t + \frac{h^2}{4t}. \quad (3.15)$$

3. $\varphi = \pi$ case

For this case Eq.(3.1b) is automatically solved and the remaining equations are

$$-2t(g+t)\sin\theta + 2ht(1-\cos\theta) = -\lambda\sin\theta \quad (3.16a)$$

$$(g^2 - t^2)(1 + \cos\theta) - h^2(1 - \cos\theta) + 2ht\sin\theta = \lambda\cos\theta. \quad (3.16b)$$

Since Eq.(3.16) can be derived from Eq.(3.4) by changing $\theta \rightarrow -\theta$, the solutions for this case are also categorized by

$$z = \frac{g+t}{h}, \quad -\frac{r_+}{2t}, \quad -\frac{r_-}{2t}. \quad (3.17)$$

Since Eq.(3.16a) reduces to

$$\lambda = -2htz + 2t^2 + 2tg, \quad (3.18)$$

comparison of Eq.(3.18) with Eq.(3.5) shows that the Lagrange multiplier constant λ is same with the case of $\varphi = 0$. Since, furthermore, $s_x = \sin \theta \cos \varphi$ and $s_z = \cos \theta$ are invariant under $\theta \rightarrow -\theta$ and $\varphi = 0 \rightarrow \varphi = \pi$, this fact implies that the eigenvalues for this case are exactly same with those for $\varphi = 0$ case.

4. $\lambda = 2t^2 - 2gt$ case

For this case Eq.(3.1b) is automatically solved and the remaining equations are

$$2t(g+t) \sin \theta \cos \varphi + 2ht(1 - \cos \theta) = -2t(g-t) \sin \theta \cos \varphi \quad (3.19a)$$

$$(g^2 - t^2)(1 + \cos \theta) - h^2(1 - \cos \theta) - 2ht \sin \theta \cos \varphi = -2t(g-t) \cos \theta. \quad (3.19b)$$

Since Eq.(3.19a) gives a relation

$$\cos \varphi = -\frac{h}{2g} \frac{1 - \cos \theta}{\sin \theta}, \quad (3.20)$$

combining Eq.(3.19b) and Eq.(3.20) enables us to express $\cos \theta$ and $\sin \theta$ as

$$\cos \theta = -\frac{g^2 - h^2 + gt}{g^2 + h^2 + 3gt} \quad \sin \theta = \pm \frac{\sqrt{4g(g+2t)(h^2 + gt)}}{g^2 + h^2 + 3gt}. \quad (3.21)$$

For a time being we choose the upper sign in $\sin \theta$. Then, Eq.(3.20) reduces to

$$\cos \varphi = \frac{h}{2} \sqrt{\frac{g+2t}{g(h^2 + gt)}}. \quad (3.22)$$

At this stage it is worthwhile noting that the eigenvalue in this case is available when

$$(3g - 2t)h^2 + 4g^2t \geq 0 \quad (3.23)$$

because of $-1 \leq \cos \varphi \leq 1$. Of course, the corresponding $\sin \varphi$ is

$$\sin \varphi = \pm \sqrt{\frac{3gh^2 + 4g^2t - 2h^2t}{4g(h^2 + gt)}}. \quad (3.24)$$

Again we choose the upper sign in $\sin \varphi$. Then, it is straightforward to compute \mathbf{s} , whose components are

$$s_x = -\frac{h(g+2t)}{g^2 + h^2 + 3gt} \quad s_y = \frac{\sqrt{(g+2t)(3gh^2 + 4g^2t - 2h^2t)}}{g^2 + h^2 + 3gt} \quad s_z = -\frac{g^2 - h^2 + gt}{g^2 + h^2 + 3gt}. \quad (3.25)$$

Inserting Eq.(3.25) into Eq.(2.4) gives the eigenvalue for this case as follows:

$$\mu_2^2 = \frac{g(gh^2 + 4t^3)}{g^2 + h^2 + 3gt}. \quad (3.26)$$

It is easy to show that the choice of other sign in $\sin \theta$ and $\sin \varphi$ does not change the eigenvalue μ_2^2 .

The eigenvalues for $\gamma = 0$ case are summarized in Table I.

name	eigenvalue	λ	available region
μ_P^2	g^2	$2(g^2 - t^2)$	all
μ_1^2	$\frac{g^2 h^2 + t^2 (g+t)^2}{h^2 + (g+t)^2}$	0	all
μ_+^2	$\frac{(hr_+ + 4t^2)^2}{r_+^2 + 4t^2}$	$hr_+ + 2t(g+t)$	$g \leq 2t + h^2/(4t)$
μ_-^2	$\frac{(hr_- + 4t^2)^2}{r_-^2 + 4t^2}$	$hr_- + 2t(g+t)$	$g \leq 2t + h^2/(4t)$
μ_2^2	$\frac{g(gh^2 + 4t^3)}{g^2 + h^2 + 3gt}$	$2t(t - g)$	$(3g - 2t)h^2 + 4g^2t \geq 0$

Table I: Eigenvalues for $\gamma = 0$ case

B. $\gamma = \pi/2$ case

For this case Eq.(2.10) reduces to

$$2t(g+t) \sin \theta \cos \varphi = \lambda \sin \theta \cos \varphi, \quad (3.27a)$$

$$-2t(g-t) \sin \theta \sin \varphi + 2ht(1 - \cos \theta) = \lambda \sin \theta \sin \varphi, \quad (3.27b)$$

$$(g^2 - t^2)(1 + \cos \theta) - h^2(1 - \cos \theta) - 2ht \sin \theta \sin \varphi = \lambda \cos \theta. \quad (3.27c)$$

Eq.(3.27a) guarantees that the solutions for this case are categorized by $\theta = 0$, $\varphi = \pi/2$, $\varphi = 3\pi/2$ and $\lambda = 2t(g+t)$. Since the calculation procedure for the first three cases are similar to the $\gamma = 0$ case, we will briefly sketch the final result only. Although the calculation procedure for the last case is also similar to the previous case, it gives a non-trivial available region, which is important to compute the geometric measures in next section. Therefore, we will present the last case in detail.

When $\theta = 0$, the Lagrangian multiplier constant is same with Eq.(3.2) and the corresponding eigenvalue is

$$\nu_P^2 = g^2. \quad (3.28)$$

When $\varphi = \pi/2$, there are three types of solutions depending on $z = \tan(\theta/2)$. If $z = (g-t)/h$, we have vanishing Lagrange multiplier constant and the corresponding eigenvalue is

$$\nu_1^2 = \frac{g^2 h^2 + t^2 (g-t)^2}{h^2 + (g-t)^2}. \quad (3.29)$$

When $z = s_{\pm}/2t$, where

$$s_{\pm} = h \pm \sqrt{h^2 + 4t(2t+g)}, \quad (3.30)$$

the corresponding Lagrange multiplier constants are $hs_{\pm} - 2t(g-t)$, and the corresponding eigenvalues are

$$\nu_{\pm}^2 = \frac{(hs_{\pm} + 4t^2)^2}{s_{\pm}^2 + 4t^2}. \quad (3.31)$$

It should be noted that ν_{\pm}^2 are available in entire parameter space, while μ_{\pm}^2 in $\gamma = 0$ case is restricted by Eq.(3.15). As in the case of $\gamma = 0$, $\varphi = 3\pi/2$ case does not give a new eigenvalue. This case just reproduces ν_1^2 and ν_{\pm}^2 .

Finally, let us discuss $\lambda = 2t(g+t)$ case. For this case Eq.(3.27a) is automatically solved and the remaining equations are

$$2ht(1 - \cos \theta) - 2t(g-t) \sin \theta \sin \varphi = 2t(g+t) \sin \theta \sin \varphi \quad (3.32a)$$

$$(g^2 - t^2)(1 + \cos \theta) - h^2(1 - \cos \theta) - 2ht \sin \theta \sin \varphi = 2t(g+t) \cos \theta. \quad (3.32b)$$

Since Eq.(3.32a) gives a relation

$$\sin \varphi = \frac{h}{2g} \frac{1 - \cos \theta}{\sin \theta}, \quad (3.33)$$

combining Eq.(3.32b) and Eq.(3.33) yields

$$\cos \theta = -\frac{g^2 - h^2 - gt}{g^2 + h^2 - 3gt}. \quad (3.34)$$

The requirement $-1 \leq \cos \theta \leq 1$ gives first available condition

$$(g-2t)(h^2 - gt) \geq 0. \quad (3.35)$$

Now we choose $\sin \theta$ as

$$\sin \theta = \frac{\sqrt{4g(g-2t)(h^2 - gt)}}{g^2 + h^2 - 3gt}. \quad (3.36)$$

Then from Eq.(3.33) $\sin \varphi$ becomes

$$\sin \varphi = \frac{h}{2} \sqrt{\frac{g-2t}{g(h^2 - gt)}}. \quad (3.37)$$

Another requirement $-1 \leq \sin \varphi \leq 1$ gives second available condition

$$(g - 2t)(3gh^2 - 4g^2t + 2h^2t) \geq 0. \quad (3.38)$$

Choosing $\cos \varphi$ as

$$\cos \varphi = \sqrt{\frac{3gh^2 - 4g^2t + 2h^2t}{4g(h^2 - gt)}}, \quad (3.39)$$

it is straightforward to show that the eigenvalues for this case is

$$\nu_2^2 = \frac{g(gh^2 - 4t^3)}{g^2 + h^2 - 3gt}. \quad (3.40)$$

It is easy to show that the different choices in the sign of $\sin \theta$ and/or $\cos \varphi$ do not change the eigenvalue. Although the available region for ν_2^2 is restricted by Eq.(3.35) and Eq.(3.38), one can show that Eq.(3.38) implies Eq.(3.35) already. To show this explicitly let us consider $g \geq 2t$ case first. In this case Eq.(3.38) imposes $h^2 \geq 4g^2t/(3g + 2t)$. Therefore

$$h^2 - gt \geq \frac{4g^2t}{3g + 2t} - gt = \frac{gt}{3g + 2t}(g - 2t) \geq 0.$$

Similarly, one can show that Eq.(3.38) implies Eq.(3.35) for $g \leq 2t$ region too. Therefore, the available region for ν_2^2 is restricted by Eq.(3.38) only.

The eigenvalues in $\gamma = \pi/2$ case is summarized in Table II.

name	eigenvalue	λ	available region
ν_P^2	g^2	$2(g^2 - t^2)$	all
ν_1^2	$\frac{g^2h^2 + t^2(g-t)^2}{h^2 + (g-t)^2}$	0	all
ν_+^2	$\frac{(hs_+ + 4t^2)^2}{s_+^2 + 4t^2}$	$hs_+ - 2t(g - t)$	all
ν_-^2	$\frac{(hs_- + 4t^2)^2}{s_-^2 + 4t^2}$	$hs_- - 2t(g - t)$	all
ν_2^2	$\frac{g(gh^2 - 4t^3)}{g^2 + h^2 - 3gt}$	$2t(g + t)$	$(g - 2t)(3gh^2 - 4g^2t + 2h^2t) \geq 0$

Table II: Eigenvalues for $\gamma = \pi/2$ case

C. $h \rightarrow 0$ limit

Since $|\psi\rangle$ is independent of γ in the $h \rightarrow 0$ limit, all eigenvalues for $\gamma = 0$ and $\gamma = \pi/2$ cases should be same including the available region in the parameter space. Note that

$\mu_+^2 = \mu_-^2$ and $\nu_+^2 = \nu_-^2$ in the $h \rightarrow 0$ limit. In this limit the eigenvalues for $\gamma = 0$ exactly coincide with eigenvalues for $\gamma = \pi/2$ as following:

$$\mu_P^2 = \nu_P^2 = g^2 \quad \mu_1^2 = \nu_1^2 = t^2 \quad \mu_2^2 = \nu_{\pm}^2 = \frac{4t^3}{3t+g} \quad \mu_{\pm}^2 = \nu_2^2 = \frac{4t^3}{3t-g}. \quad (3.41)$$

In addition, first three eigenvalues in Eq.(3.41) are available in the full parameter space and the last one is available only at $g \leq 2t$. Thus, our calculational results are perfectly consistent in the $h \rightarrow 0$ limit.

IV. GEOMETRIC MEASURE FOR $\gamma = 0$

In this section we would like to compute the geometric entanglement measure defined

$$G(\psi) = 1 - P_{max}(\psi) \quad (4.1)$$

for $\gamma = 0$ case. In order to compute P_{max} we would like to emphasize three points, which simplify the following calculation. Firstly, note that P_{max} is given by

$$P_{max} = \max(\mu_i^2). \quad (4.2)$$

Therefore, we should choose the largest eigenvalue from all eigenvalues, each of which has its own available regions in the parameter space. Secondly, note that

$$\mu_+^2 - \mu_-^2 = \frac{128ht^{7/2}}{(r_+^2 + 4t^2)(r_-^2 + 4t^2)} \left(2t + \frac{h^2}{4t} - g \right)^{3/2}. \quad (4.3)$$

This means that μ_-^2 is always smaller than μ_+^2 in the available region $g \leq 2t + h^2/(4t)$. Therefore, we can exclude μ_-^2 from beginning for the computation of P_{max} . Thirdly, note that P_{max} is obtained from the eigenvalues whose Lagrange multiplier constants are positive[21]. This fact excludes μ_1^2 too. Considering all of these facts and available regions, it is convenient to divide the whole parameter space into the following four regions:

$$\begin{aligned} \text{(region I)} \quad & g \geq 2t + \frac{h^2}{4t} : \quad P_{max} = \mu_P^2 \\ \text{(region II)} \quad & t \leq g \leq 2t + \frac{h^2}{4t} : \quad P_{max} = \max(\mu_P^2, \mu_+^2) \\ \text{(region III)} \quad & g \leq t \ \& \ \mathcal{C}_1 \geq 0 : \quad P_{max} = \max(\mu_+^2, \mu_2^2) \\ \text{(region IV)} \quad & g \leq t \ \& \ \mathcal{C}_1 \leq 0 : \quad P_{max} = \mu_+^2 \end{aligned} \quad (4.4)$$

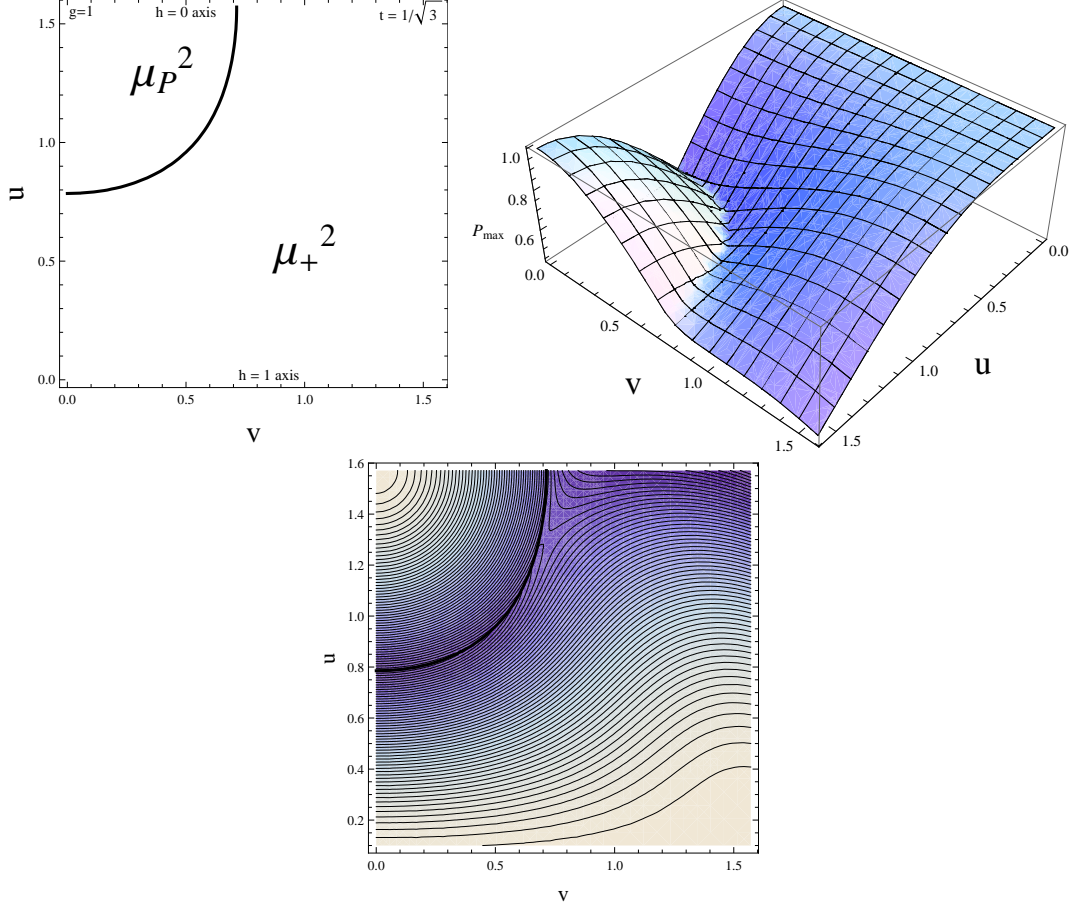


FIG. 1: (Color online) Fig. 1a is a plot of the applicable domains in (u, v) -plane for $\gamma = 0$. The principal domain $P_{max} = \mu_P^2$ is located in small v and large u region. This fact indicates that this domain is around large g region. Fig. 1b is plot of (u, v) -dependence of P_{max} for $\gamma = 0$ case. Many highly entangled states are represented as a valley in this figure. Around $u \sim 0$ and $(u \sim \pi/2, v \sim 0)$ there are a lot of less entangled states. To compare the applicable domains with P_{max} we plot both simultaneously in the (u, v) plane in Fig. 1c. The black thick line is a boundary between domains. The blue-color and white-color represent the highly- and less-entangled states respectively. Fig. 1c shows that the highly-entangled states reside around the boundary between domains.

where

$$\mathcal{C}_1 = (3g - 2t)h^2 + 4g^2t. \quad (4.5)$$

In order to compare μ_+^2 with μ_2^2 we compute $\mu_+^2 - \mu_2^2$, which is

$$\mu_+^2 - \mu_2^2 = \frac{2}{(r_+^2 + 4t^2)(g^2 + h^2 + 3gt)} \left(\alpha_1 + \beta_1 \sqrt{h^2 + 4t(2t - g)} \right) \quad (4.6)$$

where

$$\begin{aligned} \alpha_1 &= h^6 + gh^4t + 8h^4t^2 + 20gh^2t^3 + 16g^2t^4 + 4h^2t^2(2t^2 - g^2) \\ \beta_1 &= h(h^4 + 3gh^2t + 4g^2t^2 + 4h^2t^2 + 8gt^3). \end{aligned} \quad (4.7)$$

Since the last term in α_1 , $4h^2t^2(2t^2 - g^2)$, is non-negative in the region $g \leq t$, both α_1 and β_1 are non-negative in region III. In region III, therefore, P_{max} becomes μ_+^2 .

In region II it has been shown in Ref.[30] that $\mu_P^2 = \mu_+^2$ when $\mathcal{D}_1 = 0$, where

$$\mathcal{D}_1 = gh^2 - (g + t)^2(g - 2t). \quad (4.8)$$

Therefore, the region II should be divided into two regions, *i.e.* $\mathcal{D}_1 \geq 0$ and $\mathcal{D}_1 \leq 0$. Simple consideration shows that $\mu_P^2 \geq \mu_+^2$ when $\mathcal{D}_1 \leq 0$ and $\mu_P^2 \leq \mu_+^2$ when $\mathcal{D}_1 \geq 0$. Combining all of these facts, one can conclude

$$\begin{aligned} \text{(region A)} \quad & g \geq 2t + \frac{h^2}{4t} : \quad P_{max} = \mu_P^2 \\ \text{(region B)} \quad & t \leq g \leq 2t + \frac{h^2}{4t} \ \& \ \mathcal{D}_1 \leq 0 : \quad P_{max} = \mu_P^2 \\ \text{(region C)} \quad & t \leq g \leq 2t + \frac{h^2}{4t} \ \& \ \mathcal{D}_1 \geq 0 : \quad P_{max} = \mu_+^2 \\ \text{(region D)} \quad & g \leq t : \quad P_{max} = \mu_+^2. \end{aligned} \quad (4.9)$$

Now, we would like to unify the regions as many as possible to simplify the expression of P_{max} . First, one can show that \mathcal{D}_1 is always non-positive in region A as following. Since $h^2 \leq 4t(g - 2t)$ in region A, in this region

$$\mathcal{D}_1 = gh^2 - (g + t)^2(g - 2t) \leq -(g - 2t)(g - t)^2 \leq 0. \quad (4.10)$$

Second, one can show easily that \mathcal{D}_1 is always non-negative at region D as following. In this region

$$\mathcal{D}_1 = gh^2 + (g + t)^2(2t - g) \geq 0 \quad (4.11)$$

because both terms are non-negative. Combining these facts and Eq.(4.9) makes P_{max} to be expressed as

$$P_{max} = \begin{cases} \mu_P^2 & \text{when } \mathcal{D}_1 \leq 0 \\ \mu_+^2 & \text{when } \mathcal{D}_1 \geq 0. \end{cases} \quad (4.12)$$

In order to understand the behavior of P_{max} more clearly we introduce the two parameters u and v as following:

$$g = \sin u \cos v, \quad t = \sin u \sin v / \sqrt{3} \quad h = \cos u \quad (4.13)$$

with $0 \leq u, v \leq \pi/2$. Then, one can plot the applicable domains $\mathcal{D}_1 \leq 0$ and $\mathcal{D}_1 \geq 0$ in the $u - v$ plane, which is Fig. 1a. As Fig. 1a has shown, the domain for $\mathcal{D}_1 \leq 0$ is biased in the small v and large u region. This indicates that the domains for $\mathcal{D}_1 \leq 0$ is around large g region. The remaining region is the domain for $\mathcal{D}_1 \geq 0$. As will be shown in next section, the number of the applicable domains for $\gamma = \pi/2$ case is not two but three. This means that the phase factor γ has great impact in the geometric measure of entanglement.

Fig. 1b is (u, v) -dependence of P_{max} given in Eq.(4.12). At $u = 0$, which means $h = 1$, P_{max} becomes 1 because it is separable state. At $v = 0$ and $u = \pi/2$, which means that $g = 1$, P_{max} becomes 1 again. Between them there is valley, which represents the set of the highly entangled states. There is different kind of the highly entangled states around $u = v = \pi/2$. These highly entangled states are states located near W-state, $|W\rangle = (1/\sqrt{3})(|011\rangle + |101\rangle + |110\rangle)$.

In order to compare P_{max} with the applicable domains we plot P_{max} and the boundary of domains simultaneously in $u - v$ plane in Fig. 1c. In Fig. 1c the black thick line is a boundary of the domains. The thick-blue color and light-blue (or white) colors represent the highly-entangled and less-entangled states, respectively. In the right-upper corner there are many highly entangled states which are located near W-state. Another type of the highly entangled states reside near the boundary of the applicable domains. Apart from the boundary more and more the quantum states lose the entanglement, and eventually reduce to the separable state.

Now, we consider several special cases. First example is $t = 1/\sqrt{3}$ and $g = h = 0$. In this case $\mathcal{D}_1 = 2\sqrt{3}/9 > 0$ and $r_+ = \sqrt{8/3}$, which gives $P_{max} = 4/9$. Second example is $t = 0$ and $g \geq h$. In this case $\mathcal{D}_1 = -g(g^2 - h^2) \leq 0$ and $P_{max} = g^2$. Third example is $t = 0$ and $g \leq h$. In this case $\mathcal{D}_1 = g(h^2 - g^2) \geq 0$ and $r_+ = 2h$, which gives $P_{max} = h^2$. The second and third examples are consistent with $P_{max}(GHZ) = \max(|\alpha|^2, |\beta|^2)$, where $|GHZ\rangle = \alpha|000\rangle + \beta|111\rangle$. Fourth example is $g = 0$ case. In this case $\mathcal{D}_1 = 2t^3 \geq 0$ and $r_+ = h + \sqrt{h^2 + 8t^2}$, which results in

$$P_{max} = \frac{(h^4 + 8h^2t^2 + 8t^4) + h(h^2 + 4t^2)\sqrt{h^2 + 8t^2}}{(h^2 + 6t^2) + h\sqrt{h^2 + 8t^2}}. \quad (4.14)$$

One can show that various limits of Eq.(4.14) are consistent with the previously derived results. The last example is $h = 0$ case. In this case it is easy to show

$$P_{max} = \begin{cases} g^2 & \text{when } g \geq 2t \\ 4t^3/(3t - g) & \text{when } g \leq 2t. \end{cases} \quad (4.15)$$

Eq.(4.15) is perfectly in agreement with the result of Ref.[22].

V. GEOMETRIC MEASURE FOR $\gamma = \pi/2$

In this section we would like to compute the geometric entanglement measure for $\gamma = \pi/2$ case. From the constraint of the positive Lagrange multiplier constant we can exclude ν_1^2 and ν_-^2 from beginning stage for the computation of the geometric measure. Next, we should examine the sign of the Lagrange multiplier constant for ν_+^2 , that is

$$\lambda_+ = hs_+ - 2t(g - t). \quad (5.1)$$

It is easy to show that $\lambda_+ \geq 0$ in $g \leq t$ region. Also it is straightforward to show that $\lambda_+ \geq 0$ when $\mathcal{C}_+ \geq 0$ and $\lambda_+ \leq 0$ when $\mathcal{C}_+ \leq 0$, where

$$\mathcal{C}_+ = h^2(2g + t) - t(g - t)^2. \quad (5.2)$$

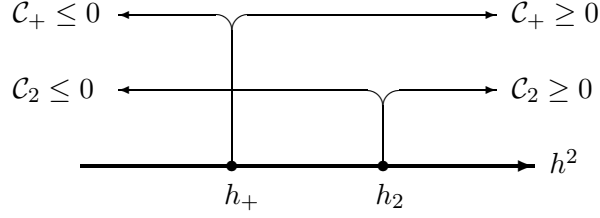


FIG. 2: Pictorial representation for $C_2 \geq 0$, $C_2 \leq 0$, $C_+ \geq 0$, and $C_+ \leq 0$ when $g \geq t$.

Examining Table II and Eq.(5.2) leads us to divide the whole parameter space into the following ten regions:

$$(i) \quad g \geq 2t \quad (5.3)$$

$$\text{(region I)} \quad C_2 \leq 0 \ \& \ C_+ \leq 0 : \quad P_{max} = \nu_P^2$$

$$\text{(region II)} \quad C_2 \geq 0 \ \& \ C_+ \leq 0 : \quad P_{max} = \max(\nu_P^2, \nu_2^2)$$

$$\text{(region III)} \quad C_2 \leq 0 \ \& \ C_+ \geq 0 : \quad P_{max} = \max(\nu_P^2, \nu_+^2)$$

$$\text{(region IV)} \quad C_2 \geq 0 \ \& \ C_+ \geq 0 : \quad P_{max} = \max(\nu_P^2, \nu_+^2, \nu_2^2)$$

$$(ii) \quad t \leq g \leq 2t$$

$$\text{(region V)} \quad C_2 \geq 0 \ \& \ C_+ \leq 0 : \quad P_{max} = \nu_P^2$$

$$\text{(region VI)} \quad C_2 \leq 0 \ \& \ C_+ \leq 0 : \quad P_{max} = \max(\nu_P^2, \nu_2^2)$$

$$\text{(region VII)} \quad C_2 \geq 0 \ \& \ C_+ \geq 0 : \quad P_{max} = \max(\nu_P^2, \nu_+^2)$$

$$\text{(region VIII)} \quad C_2 \leq 0 \ \& \ C_+ \geq 0 : \quad P_{max} = \max(\nu_P^2, \nu_+^2, \nu_2^2)$$

$$(iii) \quad g \leq t$$

$$\text{(region IX)} \quad C_2 \leq 0 : \quad P_{max} = \max(\nu_+^2, \nu_2^2)$$

$$\text{(region X)} \quad C_2 \geq 0 : \quad P_{max} = \nu_+^2$$

where

$$C_2 = (3g + 2t)h^2 - 4g^2t. \quad (5.4)$$

Although the whole space is divided into the ten regions, one can show that some regions do not exist. In order to show this it is convenient to introduce

$$h_2 = \frac{4g^2t}{3g + 2t} \quad h_+ = \frac{t(g-t)^2}{2g+t}. \quad (5.5)$$

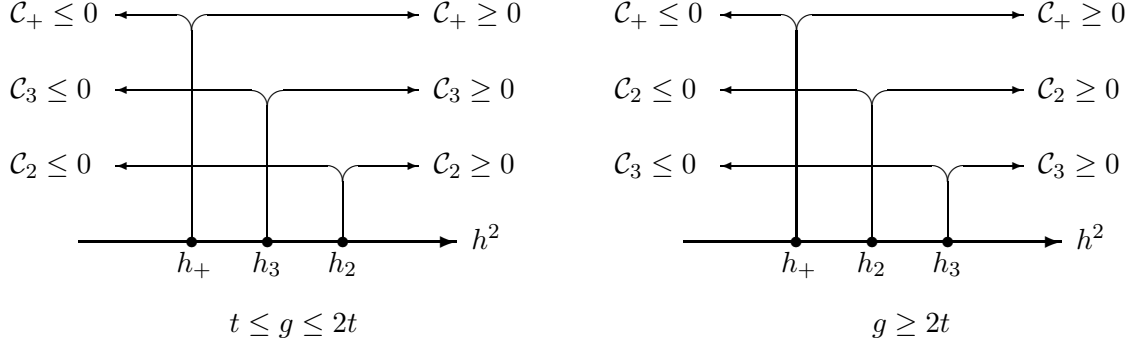


FIG. 3: Pictorial representation for $\mathcal{C}_2 \geq 0$, $\mathcal{C}_2 \leq 0$, $\mathcal{C}_+ \geq 0$, $\mathcal{C}_+ \leq 0$, $\mathcal{C}_3 \geq 0$ and $\mathcal{C}_3 \leq 0$ when $t \leq g \leq 2t$ (Fig. 2 a) and $g \geq 2t$ (Fig. 2 b).

Then, their difference becomes

$$h_2 - h_+ = \frac{t(g+t)^2}{(3g+2t)(2g+t)}(5g-2t). \quad (5.6)$$

Eq.(5.6) implies that $h_2 \geq h_+$ in the region $g \geq t$. Then the regions $\mathcal{C}_2 \geq 0$, $\mathcal{C}_2 \leq 0$, $\mathcal{C}_+ \geq 0$, and $\mathcal{C}_+ \leq 0$ when $g \geq t$ can be represented as Fig. 2. With an help of Fig. 2 it is easy to understand that there is no region which satisfies both $\mathcal{C}_2 \geq 0$ and $\mathcal{C}_+ \leq 0$ when $g \geq t$. This implies that region II and region V do not exist in the whole parameter space.

In order to compare ν_P^2 with ν_2^2 we compute $\nu_P^2 - \nu_2^2$, which is

$$\nu_P^2 - \nu_2^2 = \frac{g(g+t)(g-2t)^2}{g^2 + h^2 - 3gt}. \quad (5.7)$$

Therefore, the sign of $\nu_P^2 - \nu_2^2$ is determined by $g^2 + h^2 - 3gt$. If $\mathcal{C}_2 \geq 0$, $h^2 \geq h_2$ and

$$g^2 + h^2 - 3gt \geq \frac{3g(g-2t)(g+t)}{3g+2t}. \quad (5.8)$$

Therefore, if $\mathcal{C}_2 \geq 0$ in $g \geq 2t$ region, $\nu_P^2 \geq \nu_2^2$. Thus, we can exclude ν_2^2 in region IV. Similarly, one can show that if $\mathcal{C}_2 \leq 0$ in $t \leq g \leq 2t$ region, $\nu_P^2 \leq \nu_2^2$. Therefore, we can exclude ν_P^2 in regions VI and VIII.

Next, we compute $\nu_P^2 - \nu_+^2$, which is

$$\nu_P^2 - \nu_+^2 = \frac{2}{s_+^2 + 4t^2} \left(\alpha_2 + \beta_2 \sqrt{h^2 + 4t(2t+g)} \right) \quad (5.9)$$

where

$$\begin{aligned}\alpha_2 &= -h^4 + (g + 2t)(g - 4t)h^2 + 2t(g - t)(g + 2t)^2 \\ \beta_2 &= h(g^2 - h^2 - 4t^2).\end{aligned}\tag{5.10}$$

Direct calculation shows that in $g \geq t$ region $\nu_P^2 = \nu_+^2$ when $\mathcal{C}_3 = 0$, where

$$\mathcal{C}_3 = gh^2 - (g - t)^2(g + 2t).\tag{5.11}$$

In addition, simple consideration shows that in $g \geq t$ region $\nu_P^2 \geq \nu_+^2$ when $\mathcal{C}_3 \leq 0$ and $\nu_P^2 \leq \nu_+^2$ when $\mathcal{C}_3 \geq 0$.

In order to check which eigenvalue is dominant in each region it is convenient to introduce another parameter

$$h_3 = \frac{(g - t)^2(g + 2t)}{g}.\tag{5.12}$$

Then, it is easy to show

$$\begin{aligned}h_+ &\leq h_2 \leq h_3 && \text{when } 2t \leq g \\ h_+ &\leq h_3 \leq h_2 && \text{when } t \leq g \leq 2t.\end{aligned}\tag{5.13}$$

Eq.(5.13) enables us to represent $\mathcal{C}_2 \geq 0$, $\mathcal{C}_2 \leq 0$, $\mathcal{C}_+ \geq 0$, $\mathcal{C}_+ \leq 0$, $\mathcal{C}_3 \geq 0$ and $\mathcal{C}_3 \leq 0$ in one-dimensional coordinate, which is illustrated in Fig. 3. With an help of Fig. 3 one can show easily that in region III \mathcal{C}_3 is always non-positive and therefore, P_{max} becomes ν_P^2 . Using Fig. 3a P_{max} in region VII is ν_+^2 . Using Fig. 3b again one can show that region IV is divided into

$$\begin{aligned}(\text{region IV-a}) \quad \mathcal{C}_2 \geq 0 \ \& \ \mathcal{C}_3 \leq 0 : \quad P_{max} = \nu_P^2 \\ (\text{region IV-b}) \quad \mathcal{C}_2 \geq 0 \ \& \ \mathcal{C}_3 \geq 0 : \quad P_{max} = \nu_+^2.\end{aligned}\tag{5.14}$$

Finally, we compute $\nu_+^2 - \nu_2^2$, which is

$$\nu_+^2 - \nu_2^2 = \frac{2}{(s_+^2 + 4t^2)(g^2 + h^2 - 3gt)} \left(\alpha_3 + \beta_3 \sqrt{h^2 + 4t(2t + g)} \right)\tag{5.15}$$

where

$$\begin{aligned}\alpha_3 &= h^6 + t(8t - g)h^4 - 4t^2(g^2 + 5gt - 2t^2)h^2 + 16g^2t^4 \\ \beta_3 &= h [h^4 + t(4t - 3g)h^2 + 4gt^2(g - 2t)].\end{aligned}\tag{5.16}$$

One can show directly that $\nu_+^2 - \nu_2^2 = 0$ when $\mathcal{C}_2 = 0$. Also, it is straightforward to show that in $g \leq 2t$ region ν_+^2 is always smaller than ν_2^2 . Therefore, we can exclude ν_+^2 in regions VIII and IX. Combining all of these facts, one can express P_{max} for $\gamma = \pi/2$ case as follows:

$$\begin{aligned}
& (i) \quad g \geq 2t \tag{5.17} \\
P_{max} &= \begin{cases} \nu_+^2 & \mathcal{C}_2 \geq 0 \ \& \ \mathcal{C}_3 \geq 0 \\ \nu_P^2 & \text{remaining region} \end{cases} \\
& (i) \quad g \leq 2t \\
P_{max} &= \begin{cases} \nu_+^2 & \mathcal{C}_2 \geq 0 \\ \nu_2^2 & \mathcal{C}_2 \leq 0. \end{cases}
\end{aligned}$$

Unlike $\gamma = 0$ case the whole parameter space is divided into the three applicable domains. Introducing the parameters u and v as Eq.(4.13) we plot the three applicable domains in the u - v plane in Fig. 4a. Around $h = 0$ axis there are two domains, *i.e.* ν_P^2 and ν_2^2 . Since ν_P^2 and ν_2^2 go to μ_P^2 and μ_+^2 in the $h \rightarrow 0$ limit, this guarantees that the $h \rightarrow 0$ limit is consistent with same limit of $\gamma = 0$ case. The applicable domain for ν_P^2 is little bit larger than the domain μ_P^2 for $\gamma = 0$ case. The point $(u = \cos^{-1}(\sqrt{2}/3), v = \tan^{-1}(\sqrt{3}/2))$ is shared by three domains. This point corresponds to

$$|\psi_W\rangle = \frac{2}{3}|000\rangle + \frac{1}{3}(|011\rangle + |101\rangle + |110\rangle) + i\frac{\sqrt{2}}{3}|111\rangle. \tag{5.18}$$

This is LU-equivalent with $|W\rangle = (1/\sqrt{3})(|100\rangle + |010\rangle + |001\rangle)$ as shown in Ref.[30].

In Fig. 4b we plot the (u, v) -dependence of P_{max} given in Eq.(5.17). Like Fig. 1b the highly entangled states are represented as a valley in this figure. Fig. 4b seems to show that there exists an alley in the valley, which ends at $u = v = \pi/2$. Along this alley so many highly entangled states are located. Comparing Fig. 4b with Fig. 1b, one can realize that there are many more highly-entangled states for $\gamma = \pi/2$ case than $\gamma = 0$ case. This is mainly due to the fact that there are two LU-equivalent W-states when $\gamma = \pi/2$.

Fig. 4c shows the geometric entanglement measure and the applicable domains simultaneously in the u - v plane. Fig. 4c shows that around two W-states there are so many highly entangled states, which we would like to call W-neighbors. Especially, the neighbors of $|\psi_W\rangle$ in Eq.(5.18) gather along $\mathcal{C}_3 = 0$ line. Besides the W-neighbors there are many highly entangled states around boundary of the applicable domains. These are the neighbors of the shared states[22], and we would like to call them the GHZ-neighbors. The GHZ-neighbors

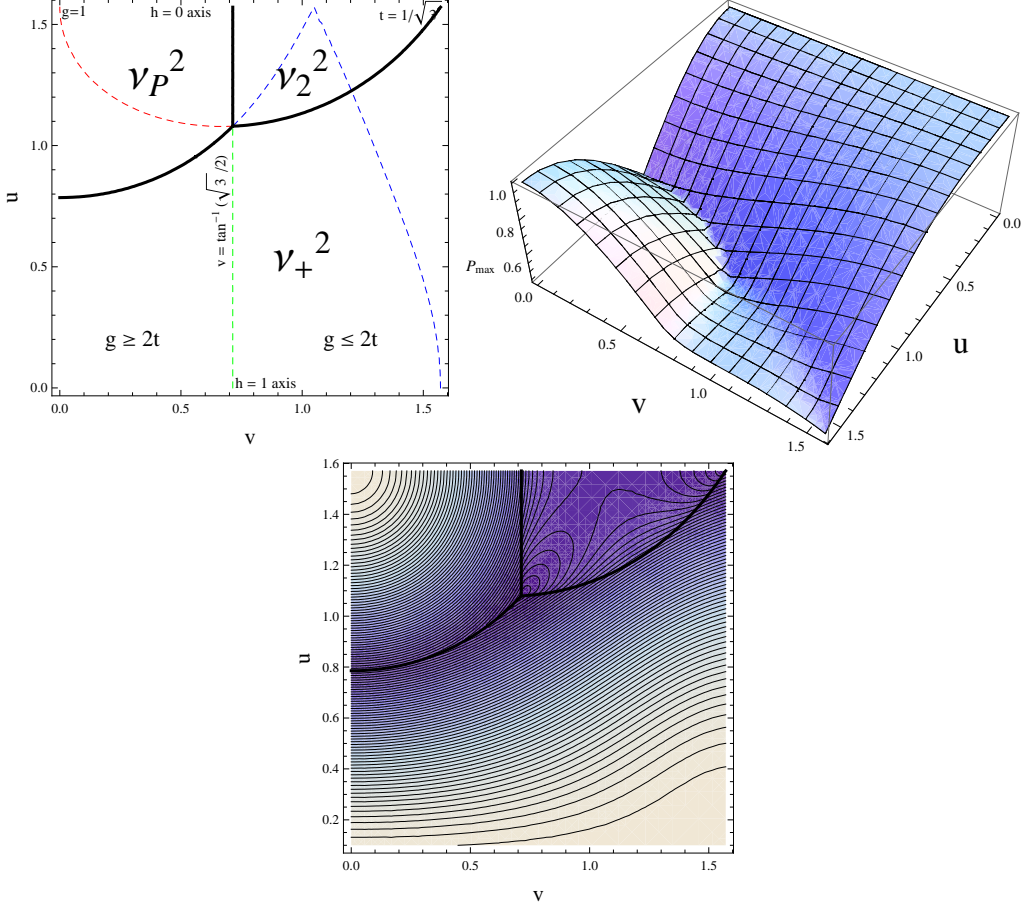


FIG. 4: (Color online) Fig. 4(a) is a plot of the applicable domains for $\gamma = \pi/2$ case in (u, v) -plane. Unlike $\gamma = 0$ case there are three applicable domains in this case. The principal domain $P_{max} = \nu_P^2$ is larger than $P_{max} = \mu_P^2$ in $\gamma = 0$ case. This fact seems to indicate that the principal domain increases its territory with increasing γ . It is important to note that the domain $P_{max} = \nu_+^2$ is not reached to $h = 0$ axis. This implies the consistency of the $h \rightarrow 0$ limit. Fig. 4(b) is (u, v) -dependence of P_{max} . The highly entangled states forms a valley between two mountains. Fig. 4(c) is a plot of P_{max} and the applicable domains in the (u, v) -plane. The boundaries of the domains are represented by black thick line. Many highly-entangles states reside around the boundaries and in the domain $P_{max} = \nu_+^2$. It is mainly due to the fact that there are two LU-equivalent W-states for $\gamma = \pi/2$ case.

are slightly less-entangled compared to the W-neighbors. However, the number of the GHZ-neighbors are many more than that of the W-neighbors.

Finally, we consider the several special cases. First example is $h = 0$ case. In this case $\mathcal{C}_2 = -4g^2t \leq 0$ and $\mathcal{C}_3 = -(g-t)^2(g+2t) \leq 0$, which results in identical expression with Eq.(4.15). Therefore, both results for $\gamma = 0$ and $\gamma = \pi/2$ cases coincide with each other in the $h \rightarrow 0$ limit. Second example is $t = 0$ case. It is easy to show that in this case $P_{max} = g^2$ when $g \geq h$ and $P_{max} = h^2$ when $g \leq h$. This is consistent with $P_{max}(GHZ) = \max(|\alpha|^2, |\beta|^2)$ when $|GHZ\rangle = \alpha|000\rangle + |\beta|111\rangle$.

VI. EIGENVALUES AND GEOMETRIC MEASURE FOR $\gamma = \pi/4$: NUMERICAL APPROACH

In this section we will compute the eigenvalues and the geometric measure for $\gamma = \pi/4$ case.

A. Eigenvalues

For $\gamma = \pi/4$ Eq.(2.10) reduces to

$$2t(g+t)\sin\theta\cos\varphi + \sqrt{2}ht(1-\cos\theta) = \lambda\sin\theta\cos\varphi \quad (6.1a)$$

$$-2t(g-t)\sin\theta\sin\varphi + \sqrt{2}ht(1-\cos\theta) = \lambda\sin\theta\sin\varphi \quad (6.1b)$$

$$(g^2-t^2)(1+\cos\theta) - h^2(1-\cos\theta) - \sqrt{2}ht\sin\theta(\sin\varphi+\cos\varphi) = \lambda\cos\theta. \quad (6.1c)$$

When $\theta = 0$, Eq.(6.1a) and Eq.(6.1b) are automatically solved and Eq.(6.1c) gives

$$\lambda = 2(g^2 - t^2). \quad (6.2)$$

Since $\mathbf{s} = (0, 0, 1)$ for this case, from Eq.(2.4) the corresponding eigenvalue is

$$\rho_P^2 = g^2. \quad (6.3)$$

When $\sin\theta \neq 0$, Eq.(6.1a) and Eq.(6.1b) reduce to

$$z = \frac{\lambda - 2gt - 2t^2}{\sqrt{2}ht} \cos\varphi = \frac{\lambda + 2gt - 2t^2}{\sqrt{2}ht} \sin\varphi \quad (6.4)$$

where $z = \tan(\theta/2)$. From Eq.(6.4) one can compute φ if λ is known by using

$$\tan\varphi = \frac{(\lambda - 2t^2) - 2gt}{(\lambda - 2t^2) + 2gt}. \quad (6.5)$$

Deriving $\sin \varphi + \cos \varphi$ from Eq.(6.4) and inserting it into Eq.(6.1c), one can derive the expression of z^2 in a form

$$z^2 = \frac{[(\lambda - 2t^2)^2 - 4g^2t^2](\lambda - 2g^2 + 2t^2)}{(\lambda - 2h^2)(\lambda - 2t^2)^2 - 8h^2t^2(\lambda - 2t^2) - 4g^2t^2(\lambda - 2h^2)}. \quad (6.6)$$

On the other hand, one can derive a different expression of z^2 directly from Eq.(6.4)

$$z^2 = \frac{(\lambda - 2gt - 2t^2)^2}{2h^2t^2}(1 + \tan^2 \varphi)^{-1} = \frac{[(\lambda - 2t^2)^2 - 4g^2t^2]^2}{4h^2t^2[(\lambda - 2t^2)^2 + 4g^2t^2]}. \quad (6.7)$$

Equating Eq.(6.6) with Eq.(6.7) yields an equation for solely λ :

$$\lambda f(\lambda) = 0 \quad (6.8)$$

where

$$\begin{aligned} f(\lambda) = & \lambda^4 - 2(h^2 + 4t^2)\lambda^3 - 4t^2(2g^2 - h^2 - 6t^2)\lambda^2 \\ & + 8[t^4(h^2 - 4t^2) + g^2(3h^2t^2 + 4t^4)]\lambda \\ & + 16t^4(g^4 - 5g^2h^2 - 2g^2t^2 - h^2t^2 + t^4). \end{aligned} \quad (6.9)$$

Eq.(6.8) guarantees the existence of the eigenvalue for $\lambda = 0$ as $\gamma = 0$ and $\gamma = \pi/2$ cases. In fact, one can show that there exists an eigenvalue corresponding to $\lambda = 0$ for arbitrary γ . We have shown this fact in appendix A.

When $\lambda = 0$, Eq.(6.5) and Eq.(6.7) reduce to

$$z^2 = \frac{(g^2 - t^2)^2}{h^2(g^2 + t^2)} \quad \tan \varphi = -\frac{g + t}{g - t}. \quad (6.10)$$

Combining Eq.(6.4) and Eq.(6.10), the possible solutions for θ and φ are

$$z = \pm \frac{g^2 - t^2}{h\sqrt{g^2 + t^2}} \quad \cos \varphi = \mp \frac{g - t}{\sqrt{2(g^2 + t^2)}} \quad \sin \varphi = \pm \frac{g + t}{\sqrt{2(g^2 + t^2)}}. \quad (6.11)$$

It is easy to show that both solutions in Eq.(6.11) gives a same eigenvalue, which is

$$\rho_0^2 = \frac{g^2(g^2 + t^2)h^2 + t^2(g^2 - t^2)^2}{h^2(g^2 + t^2) + (g^2 - t^2)^2}. \quad (6.12)$$

Finally, let us consider $f(\lambda) = 0$. It is worthwhile noting that at $h \rightarrow 0$ limit $f(\lambda) = 0$ reduces to $(\lambda - 2gt - 2t^2)^2(\lambda + 2gt - 2t^2)^2 = 0$. Therefore, the eigenvalues corresponding to $f(\lambda) = 0$ should coincide with μ_{\pm}^2 and μ_2^2 for $\gamma = 0$ case, and with ν_{\pm}^2 and ν_2^2 for $\gamma = \pi/2$ case at the $h \rightarrow 0$ limit. Equation $f(\lambda) = 0$ gives four solutions of λ , say $\lambda_1, \lambda_2, \lambda_3$ and λ_4 . We ordered the solutions by a fact that the $h \rightarrow 0$ limit of λ_1 and λ_2 is $-2t(g - t)$ and same limit of λ_3 and λ_4 is $2t(g + t)$. Then, the corresponding eigenvalues, say $\rho_1^2, \rho_2^2, \rho_3^2$, and ρ_4^2 , can be computed numerically.

B. geometric measure

FIG. 5: (Color online) Fig. 5(a) is a plot of the applicable domains for $\gamma = \pi/4$ case. In this case there are two applicable domains. The principal domain $P_{max} = \rho_P^2$ is little bit larger than $P_{max} = \mu_P^2$ for $\gamma = 0$ and little bit smaller than $P_{max} = \nu_P^2$ for $\gamma = \pi/2$. This fact indicates that the principal domain increases its territory with increasing γ . Fig. 5(b) is (u, v) -dependence of P_{max} . As $\gamma = 0$ case the highly-entangled states form a valley between two mountains. Fig. 5(c) is a plot of P_{max} and the applicable domains in the (u, v) -plane. Many highly-entangled states reside around boundary of the domains and near W-state.

Using eigenvalues ρ_P^2 , ρ_0^2 derived analytically and ρ_i^2 ($i = 1, 2, 3, 4$) computed numerically, one can compute P_{max} for the $\gamma = \pi/4$ case. Since each eigenvalue has its own available region, we checked this region by imposing $\text{Re}[\lambda] = 0$, $-1 \leq \sin \theta \leq 1$, $-1 \leq \cos \theta \leq 1$, $-1 \leq \sin \varphi \leq 1$, and $-1 \leq \cos \varphi \leq 1$. Although there are six different eigenvalues, the numerical calculation shows that only ρ_P^2 and ρ_4^2 contribute to the geometric measure. This indicates that the whole parameter space is divided into two applicable domains. These two domains are represented in $u - v$ plane in Fig. 5a. The domains ρ_P^2 is slightly larger than domain μ_P^2 and slightly smaller than domain ν_P^2 . This fact seems to indicate that the domain containing $g = 1$ extends its territory with increasing γ .

Fig. 5b is a (u, v) -dependence of P_{max} for $\gamma = \pi/4$. Similarly with $\gamma = 0$ and $\pi/2$ cases, many highly entangled states reside at the valley between two mountains. Another highly entangled states reside around $u = v = \pi/2$, which corresponds to W-state. The alley appeared in Fig. 4b does not appear in this case. This seems to be due to the fact that there is only one W-state in $\gamma = \pi/4$ case.

Fig. 5c is a (u, v) -dependence of P_{max} and domains. As expected the highly entangled states are located around boundary and W-state.

VII. CONCLUSION

In this paper we have explored the effect of the phase factor in the geometric entanglement measure. We have chosen the most general three-qubit states which have symmetry under

the qubit-exchange. Our choice of the quantum states enables us to derive all eigenvalues and geometric measure analytically when the phase factor γ is 0 or $\pi/2$. It turns out that the $\gamma = \pi/2$ case has three applicable domains while the $\gamma = 0$ case has two domains. Most highly entangled states reside around the boundaries of the domains and near W-state. Apart from the boundaries more and more the quantum states lose their entanglement and eventually, become the product states.

Our result naturally gives rise to a question: what is a critical γ , *say* γ_c , which distinguish the two and three domains? In order to explore this question we have analyzed the $\gamma = \pi/4$ case numerically. Our numerical calculation shows that there are six different eigenvalues for $\gamma = \pi/4$ case, but only two of them contribute to the geometric entanglement measure. Thus, there are two domains for $\gamma = \pi/4$.

We conjecture that emergence of the three applicable domains at $\gamma = \pi/2$ is due to the two LU-equivalent W-states. In order to confirm our conjecture we checked numerically $\gamma = \pi/3$ and $\gamma = 11\pi/24$ cases, which also give two applicable domains. We also checked the applicable domains for the partially symmetric quantum state

$$|\psi\rangle = g|000\rangle + t|011\rangle + t|101\rangle + t_3|110\rangle + e^{i\gamma}h|111\rangle \quad (7.1)$$

numerically when $\gamma = 0$. This case also gives two applicable domains. Therefore, we conclude that the emergence of the three applicable domains is due to the appearance of additional W-state.

In appendix we have shown that there exist eigenvalues for all γ , whose Lagrangian multiplier constant is zero. Although we conjecture that this is due to some symmetry of the quantum state $|\psi\rangle$, we do not know the exact physical reason for the emergence of these solutions. It seems to be of interest to reveal the physical meaning of these solutions clearly.

Acknowledgement: This work was supported by National Research Foundation of Korea Grant funded by the Korean Government (2009-0073997).

-
- [1] R. F. Werner, *Quantum states with Einstein-Podolsky-Rosen correlations admitting a hidden-variable model*, Phys. Rev. A **40**, 4277(1989).
 [2] A. K. Ekert, *Quantum cryptography based on Bell's theorem*, Phys. Rev. Lett. **67**, 661(1991).

- [3] C. H. Bennett and S. J. Wiesner, *Communication via one- and two-particle operators on Einstein-Podolsky-Rosen states*, Phys Rev. Lett. **69**, 2881(1992).
- [4] C. H. Bennett, G. Brassard, C. Crépeau, R. Jozsa, A. Peres, and W. K. Wootters, *Teleporting an unknown quantum state via dual classical and Einstein-Podolsky-Rosen channels*, Phys. Rev. Lett. **70**, 1895(1993).
- [5] F. Casagrande, A. Lulli, and M. G. A. Paris, *Tripartite entanglement transfer from flying modes to localized qubits*, Phys. Rev. A **79**, 022307 (2009).
- [6] C. H. Bennett, H. J. Bernstein, S. Popescu, and B. Schumacher, *Concentrating partial entanglement by local operations*, Phys. Rev. A **53**, 2046 (1996).
- [7] C. H. Bennett, D. P. DiVincenzo, J. A. Smolin and W. K. Wootters, *Mixed-state entanglement and quantum error correction*, Phys. Rev. A **54**, 3824(1996).
- [8] W. K. Wootters, *Entanglement of Formation of an Arbitrary State of Two Qubits*, Phys. Rev. Lett. **80**, 2245 (1998).
- [9] G. Vidal and J. I. Cirac, *Irreversibility in Asymptotic Manipulations of Entanglement*, Phys. Rev. Lett. **86**, 5803(2001).
- [10] V. Vedral, M. B. Plenio, M. A. Rippin, and P. L. Knight, *Quantifying Entanglement*, Phys. Rev. Lett. **78**, 2275(1997).
- [11] M. B. Plenio and V. Vedral, *Bounds on relative entropy of entanglement for multi-party systems*, J. Phys. A: Math. Gen. **34**, 6997(2001).
- [12] D. A. Meyer and N. R. Wallach, *Global entanglement in multiparticle systems*, J. Math. Phys. **43**, 4273(2002).
- [13] O. Biham, M. A. Nielsen and T. J. Osborne, *Entanglement monotone derived from Grover's algorithm*, Phys. Rev. A **65**, 062312(2002).
- [14] D. Shapira, Y. Shimoni, and O. Biham, *Groverian measure of entanglement for mixed states*, Phys. Rev. A **73**, 044301(2006).
- [15] A. Shimony, *Degree of entanglement*, A conference held in honor of J. A. Wheeler, Ann. N. Y. Acad. Sci. **755**, 675 (1995).
- [16] H. Barnum and N. Linden, *Monotones and Invariants for Multi-particle Quantum States*, J. Phys. A: Math.Gen. **34**, 6787 (2001).
- [17] T.-C. Wei and P. M. Goldbart, *Geometric measure of entanglement and application to bipartite and multipartite quantum states*, Phys. Rev. A **68** 042307 (2003).

- [18] R. Werner and A. Holevo, *Counterexample to an additivity conjecture for output purity of quantum channels*, J.Math. Phys. **43**, 4353 (2002).
- [19] L. Tamaryan, D. K. Park and S. Tamaryan, *Generalized Schmidt Decomposition based on Injective Tensor Norm*, [quant-ph/0809.1290].
- [20] J. J. Hilling and A. Sudbery, *The geometric measure of multipartite entanglement and the singular values of a hypermatrix*, arXiv:0905.2094v2 [quant-ph].
- [21] L. Tamaryan, D. K. Park and S. Tamaryan, *Analytic Expressions for Geometric Measure of Three Qubit States*, Phys. Rev. **A 77** (2008) 022325, [arXiv:0710.0571 (quant-ph)].
- [22] L. Tamaryan, D. K. Park, J. W. Son, and S. Tamaryan, *Geometric Measure of Entanglement and Shared Quantum States*, Phys. Rev. **A78** (2008) 032304, [arXiv:0803.1040 (quant-ph)].
- [23] E. Jung, M. R. Hwang, D. K. Park, L. Tamaryan and S. Tamaryan, *Three-qubit Groverian Measure*, Quant. Inf. Comp. **8** (2008) 0925, [arXiv:0803.3311 (quant-ph)].
- [24] Y. Shimoni, D. Shapira, and O. Biham, *Characterization of pure quantum states of multiple qubits using the Groverian entanglement measure*, Phys. Rev. A **69**, 062303 (2004).
- [25] M. Hayashi, D. Markham, M. Muraio, M. Owari, and S. Virmani, *Bounds on Multipartite Entangled Orthogonal State Discrimination Using Local Operations and Classical Communication*, Phys. Rev. Lett. **96**, 040501 (2006).
- [26] O. Gühne, F. Bodoky, and M. Blaauboer, *Multiparticle entanglement under the influence of decoherence*, Phys. Rev. A **78**, 060301(R) (2008).
- [27] L. Tamaryan, H. Kim, E. Jung, M.-R. Hwang, D.K. Park, and S. Tamaryan, *Toward an understanding of entanglement for generalized n -qubit W -states*, arXiv:0806.1314v1[quant-ph].
- [28] A. Acín, A. Andrianov, L. Costa, E. Jané, J. I. Latorre, and R. Tarrach, *Generalized Schmidt decomposition and classification of three-quantum-bit states*, Phys. Rev. Lett. **85**, 1560(2000).
- [29] H. A. Carteret, A. Higuchi, and A. Sudbery, *Multipartite generalisation of the Schmidt decomposition*, J. Math. Phys. **41**, 7932 (2000).
- [30] S. Tamaryan, T. C. Wei and D. K. Park, *Maximally entangled three-qubit states via geometric measure of entanglement*, arXiv:0905.3791 (quant-ph).
- [31] S.J. van Enk, *The joys of permutation symmetry: direct measurements of entanglement*, Phys. Rev. Lett. **102**, 190503 (2009).
- [32] G. Toth and O. Gühne, *Entanglement and permutational symmetry*, Phys. Rev. Lett. **102**, 170503 (2009).

- [33] T.-C. Wei and S. Severini, *Matrix permanent and quantum entanglement of permutation invariant states*, arXiv:0905.0012v1 [quant-ph].

Appendix A

In this appendix we would like to show the existence of the eigenvalue μ_0^2 , which corresponds to $\lambda = 0$, at arbitrary γ . When $\lambda = 0$, Eq.(2.10) reduces to

$$2ht \cos \gamma (1 - \cos \theta) + 2t(g+t) \sin \theta \cos \varphi = 0 \quad (\text{A.1a})$$

$$2ht \sin \gamma (1 - \cos \theta) - 2t(g-t) \sin \theta \sin \varphi = 0 \quad (\text{A.1b})$$

$$(g^2 - t^2)(1 + \cos \theta) - h^2(1 - \cos \theta) - 2ht \sin \theta \cos(\varphi - \gamma) = 0. \quad (\text{A.1c})$$

The existence of μ_0^2 can be shown as following. First we derive θ and φ by making use of Eq.(A.1a) and Eq.(A.1b). Then we show that the solutions θ and ϕ also solve Eq.(A.1c).

Now, we consider only $\sin \theta \neq 0$ case. Then from Eq.(A.1a) and Eq.(A.1b) it is easy to derive

$$(g+t) \sin \gamma \cos \varphi + (g-t) \cos \gamma \sin \varphi = 0, \quad (\text{A.2})$$

which gives

$$\tan \varphi = -\frac{g+t}{g-t} \tan \gamma. \quad (\text{A.3})$$

Combining Eq.(A.2) and Eq.(A.3), one can derive the solution for φ , which is

$$\cos \varphi = \pm \frac{g-t}{\sqrt{(g-t)^2 + (g+t)^2 \tan^2 \gamma}} \quad \sin \varphi = \mp \frac{(g+t) \tan \gamma}{\sqrt{(g-t)^2 + (g+t)^2 \tan^2 \gamma}}. \quad (\text{A.4})$$

Inserting Eq.(A.4) into Eq.(A.1b), one can derive $\sin \theta$ in a form

$$\sin \theta = \mp \frac{2h(g^2 - t^2) \sqrt{g^2 + t^2 - 2gt \cos 2\gamma}}{h^2(g^2 + t^2 - 2gt \cos 2\gamma) + (g^2 - t^2)^2}. \quad (\text{A.5})$$

Inserting Eq.(A.4) and Eq.(A.5) into the lhs of Eq.(A.1c), one can show straightforwardly that Eq.(A.1c) is solved already by Eq.(A.4) and Eq.(A.5). This guarantees the existence of μ_0^2 .

In order to derive μ_0^2 explicitly we choose the upper sign in Eq.(A.4) and Eq.(A.5). Then the components of the vector \mathbf{s} becomes

$$s_x = \sin \theta \cos \varphi = \frac{-2h(g-t)^2(g+t) \cos \gamma}{h^2[(g^2 + t^2) - 2gt \cos 2\gamma] + (g^2 - t^2)^2} \quad (\text{A.6a})$$

$$s_y = \sin \theta \sin \varphi = \frac{2h(g-t)(g+t)^2 \sin \gamma}{h^2[(g^2 + t^2) - 2gt \cos 2\gamma] + (g^2 - t^2)^2} \quad (\text{A.6b})$$

$$s_z = \cos \theta = \frac{h^2[(g^2 + t^2) - 2gt \cos 2\gamma] - (g^2 - t^2)^2}{h^2[(g^2 + t^2) - 2gt \cos 2\gamma] + (g^2 - t^2)^2}. \quad (\text{A.6c})$$

Inserting Eq.(A.6) into Eq.(2.4) and performing tedious calculation, one can show that μ_0^2 , eigenvalue corresponding to $\lambda = 0$, becomes

$$\mu_0^2 = \frac{g^2 h^2 (g^2 + t^2 - 2gt \cos 2\gamma) + t^2 (g^2 - t^2)^2}{h^2 (g^2 + t^2 - 2gt \cos 2\gamma) + (g^2 - t^2)^2}. \quad (\text{A.7})$$

It is straightforward to show that the choice of lower sign in Eq.(A.4) and Eq.(A.5) leads us to same expression of μ_0^2 . One can show easily that μ_0^2 exactly coincides with μ_1^2 in Eq.(3.11), ν_1^2 in Eq.(3.29) and ρ_0^2 in Eq.(6.12) when $\gamma = 0$, $\gamma = \pi/2$ and $\gamma = \pi/4$ respectively.

Finally, making use of explicit expression of μ_0^2 , one can derive the nearest product state $|q\rangle|q\rangle|q'\rangle$ for μ_0^2 , i.e.

$$AB \langle q|\langle q|\psi\rangle = \mu_0|q'\rangle \quad AC \langle q|\langle q'|\psi\rangle = \mu_0|q\rangle \quad BC \langle q|\langle q'|\psi\rangle = \mu_0|q\rangle \quad (\text{A.8})$$

where $|\psi\rangle$ is given in Eq.(2.3). Since \mathbf{s} is a Bloch vector of $|q\rangle\langle q|$, one can show directly

$$|q\rangle = \frac{1}{\sqrt{h^2 \ell^2 + (g^2 - t^2)^2}} [h\ell|0\rangle - (g^2 - t^2)e^{-i\eta}|1\rangle] \quad (\text{A.9})$$

where

$$\ell^2 \equiv g^2 + t^2 - 2gt \cos 2\gamma \quad \cos \eta = \frac{g-t}{\ell} \cos \gamma \quad \sin \eta = \frac{g+t}{\ell} \sin \gamma. \quad (\text{A.10})$$

Inserting Eq.(A.9) into Eq.(A.8) it is straightforward to show that $|q'\rangle$ becomes

$$|q'\rangle = \frac{1}{\mathcal{N}} [\{gh^2 \ell^2 + t(g^2 - t^2)^2 e^{2i\eta}\} |0\rangle + e^{i\eta} h(g^2 - t^2) \{(g^2 - t^2)e^{i(\gamma+\eta)} - 2\ell t\} |1\rangle] \quad (\text{A.11})$$

where \mathcal{N} is a normalization constant, which makes $|q'\rangle$ unit vector.

For $\gamma = 0$ case the nearest product state becomes

$$|q\rangle = \frac{1}{\sqrt{h^2 + (g+t)^2}} (h|0\rangle - (g+t)|1\rangle) \quad (\text{A.12})$$

$$|q'\rangle = \frac{1}{\sqrt{\{gh^2 + t(g+t)^2\}^2 + h^2(g^2 - t^2)^2}} [\{gh^2 + t(g+t)^2\} |0\rangle + h(g^2 - t^2)|1\rangle].$$

It is interesting to note that $\langle q|q'\rangle = 0$ when $\mathcal{D}_1 = 0$, where \mathcal{D}_1 is given in Eq.(4.8).

For $\gamma = \pi/2$ case $|q\rangle$ and $|q'\rangle$ becomes

$$|q\rangle = \frac{1}{\sqrt{h^2 + (g-t)^2}} (h|0\rangle + i(g-t)|1\rangle) \quad (\text{A.13})$$

$$|q'\rangle = \frac{1}{\sqrt{\{gh^2 - t(g-t)^2\}^2 + h^2(g^2 - t^2)^2}} [\{gh^2 - t(g-t)^2\} |0\rangle - ih(g^2 - t^2)|1\rangle].$$

It is interesting to note that $\langle q|q'\rangle = 0$ when $\mathcal{C}_3 = 0$, where \mathcal{C}_3 is given in Eq.(5.11).